Soil Dynamics and Earthquake Engineering 90 (2016) 240–249

Contents lists available at ScienceDirect

Soil Dynamics and Earthquake Engineering

journal homepage: www.elsevier.com/locate/soildyn

Clarifying the differences between traditional liquefaction hazard maps and probabilistic liquefaction reference parameter maps

Kevin W. Franke [a,*], Kristin J. Ulmer [a], Levi T. Ekstrom [a], Jorge F. Meneses [b]

[a] Brigham Young University, 368 Clyde Building, Provo, UT 84602, United States
[b] Group Delta Consultants, Inc., 9245 Activity Road, Suite 103, San Diego, CA 92126, United States

ARTICLE INFO

Article history:
Received 8 January 2016
Received in revised form
7 August 2016
Accepted 12 August 2016
Available online 6 September 2016

Keywords:
Liquefaction Hazard Maps
Probabilistic Liquefaction Hazard Analysis
Performance-based earthquake engineering
Performance-based reference parameter maps

ABSTRACT

Traditional liquefaction hazard maps are useful tools for preliminary engineering site assessment and policy development. However, these maps should not be used for site-specific liquefaction hazard assessment. Simplified probabilistic liquefaction analysis procedures can be used instead to perform site-specific liquefaction hazard assessment, but these procedures rely on probabilistic reference parameter maps that are not yet familiar to most engineering and geological practitioners. As a result, some professionals are questioning the differences between traditional liquefaction hazard maps and the new probabilistic reference parameter maps. This paper clarifies the differences between these two types of maps, and shows how each of these maps complements the other. New probabilistic reference parameter maps for liquefaction triggering and lateral spread displacement are developed and presented for San Diego, California, and simplified probabilistic equations necessary to use the reference parameter maps are summarized. An example map-based liquefaction triggering and lateral spread displacement analysis is performed for a representative site near San Diego Bay. Results of the analysis demonstrate that the probabilistic assessment confirms and augments the information conveyed by the traditional liquefaction hazard map.

1. Introduction

Regional mapping of liquefaction hazard (e.g., liquefaction triggering, liquefaction potential index, lateral spread displacement, free-field post-liquefaction settlement) and/or susceptibility has been performed by many researchers during the past 40 years. Beginning with the work of Youd and Hoose [1] and Youd and Perkins [2], most of these researchers began incorporating a geological approach in mapping liquefaction hazard because certain types of surficial geology and their age have been observed to correlate well to observed liquefaction susceptibility, and surficial geologic maps are typically available for most locations in the United States, as well as many locations throughout the world. As a result of these efforts, liquefaction susceptibility, triggering, and lateral spread displacement maps have become a useful preliminary assessment tool to assist owners, engineers, planners, policy-makers, and risk analysts in making informed decisions regarding their sites, and are now often used as a regulatory resource [3].

Despite the usefulness of regional liquefaction hazard maps for preliminary assessment of liquefaction hazards, these maps are not intended to be used for site-specific liquefaction hazard assessment for engineering design. Site-specific assessment of such hazards, including liquefaction triggering and lateral spread displacement, requires subsurface, site geometry, and seismic loading information pertaining to the site of interest. Recent research has suggested that a probabilistic approach to site-specific liquefaction hazard assessment (termed "probabilistic liquefaction hazard analysis" by Holzer [4]) produces more consistent estimates of liquefaction hazards across different seismic environments than conventional approaches [5–7]. To make the probabilistic approach available to a larger number of engineering practitioners, researchers have developed simplified probabilistic liquefaction triggering and lateral spread displacement analysis procedures [8–11]. These simplified probabilistic procedures require the development and use of hazard-targeted reference parameter maps for liquefaction triggering and lateral spread displacement. The values obtained from these reference parameter maps are subsequently corrected for site-specific geotechnical and topographical data to closely approximate the results that would be computed with a full probabilistic procedure at the return period(s) of interest.

With the introduction of simplified probabilistic liquefaction analysis procedures and corresponding reference parameter maps, some practitioners are beginning to question the differences

* Corresponding author.
E-mail address: kevin_franke@byu.edu (K.W. Franke).

http://dx.doi.org/10.1016/j.soildyn.2016.08.019

between these reference parameter maps and traditional liquefaction hazard maps, particularly those who are not yet familiar or comfortable with the simplified probabilistic approach. For example, a common question that is asked of the authors by engineering and geology practitioners is whether the new reference parameter maps are intended to supersede or replace existing liquefaction hazard maps. This question demonstrates a fundamental misunderstanding of what the probabilistic reference parameter maps represent and how they are different from traditional liquefaction hazard maps.

This paper explores the differences between traditional liquefaction hazard maps and probabilistic reference parameter maps, and demonstrates how they are not intended to compete with one another, but rather *complement* and *complete* one another. For this demonstration, existing liquefaction hazard maps and new probabilistic reference parameter maps (at return periods of 475 and 2475 years) for a seismically active region (San Diego, California) are presented and compared. Simplified probabilistic procedures necessary for using the new reference parameter maps are presented. A demonstrative liquefaction triggering and lateral spread displacement assessment is performed for a representative site near San Diego Bay. Through this assessment, engineers will observe how traditional liquefaction hazard maps and probabilistic reference parameter maps can be used together to provide improved understanding of the liquefaction hazards at a given site, which will aid owners, designers, planners, and stake-holders in making informed and objective design decisions. While the probabilistic reference parameter maps presented in this paper are applicable specifically to the City of San Diego, the approach presented by the paper is applicable to any location for which both traditional liquefaction hazard/susceptibility maps and probabilistic reference parameter maps are available to engineers.

While this paper specifically focuses on the liquefaction hazards of triggering and lateral spreading, other hazards including post-liquefaction settlement, loss of shear strength, and increased lateral earth pressures are also important considerations that must be taken into account by engineers. As advances in dynamic soil mechanics and probabilistic earthquake engineering lead to greater understanding and improved predictive capabilities of these phenomena, simplified assessment methods and probabilistic reference parameter maps will eventually be developed for these additional hazards through future research.

2. Liquefaction hazard mapping

Current methods for mapping liquefaction hazards generally rely heavily upon correlations with mapped surficial geologic units [1,2]. This type of mapping uses criteria that relate surface geology and depositional age to liquefaction susceptibility (i.e., the “geological approach” [4]). If a particular liquefaction map considers seismic loading in addition to geologic susceptibility correlations, then the map likely estimates liquefaction triggering hazard [12].

To quantify and map the regional potential for triggering and subsequent effects, researchers have also considered available subsurface geotechnical information as well as estimates of regional ground motions (i.e., the “geotechnical approach;” Holzer 2008). Some researchers [13–16] have incorporated available geotechnical data directly with a simplified liquefaction triggering model [17–21], but the variability of triggering potential with depth requires simplifying assumptions to quantify and represent the three-dimensional phenomenon on a two-dimensional map. The most common assumption that is applied is to map only the results from the “critical layer,” or the soil layer with the lowest computed factor of safety against liquefaction. Other researchers have avoided this problem by quantifying liquefaction triggering hazard with a different metric such as the liquefaction potential index (LPI) [22–25] or the liquefaction risk index (LRI) [26,27], both of which integrate the liquefaction triggering potential over depth to generate a single liquefaction hazard value that is easier to map, but more challenging for some engineers to interpret. Regardless of the metric used to quantify liquefaction triggering hazard, geostatistics such as kriging are required with the geotechnical approach to estimate geotechnical properties and corresponding liquefaction hazards at locations where no data are available [14,16,28].

In addition to liquefaction triggering potential, other researchers [2,16,28–31] have considered lateral spread potential to develop regional liquefaction ground deformation maps. These maps typically require the additional consideration of regional topography to estimate regional horizontal ground displacements.

Liquefaction triggering and deformation hazard maps are typically developed using a single ground motion scenario. This scenario may be defined in terms of a single seismic source, with a constant magnitude and variable source-to-site distance [28] or in terms of probabilistic ground motions corresponding to some single hazard level or return period [14]. For the latter case, in which probabilistic ground motions are used, it is important to clarify that the stated hazard level or return period associated with most liquefaction hazard maps corresponds to the ground motions used to develop the map, but not necessarily to the mapped liquefaction hazard itself. Additionally, some studies [e.g., 14, 25] have considered more than one probabilistic ground motion in the development of liquefaction hazard maps. These types of maps will be addressed in Section 3 below.

Because liquefaction hazard maps are usually developed by the regional characterization of geologically mapped units based on coarsely spaced field data, they should not be used for site-specific liquefaction hazard evaluation and engineering design [32]. To clarify this point, most liquefaction hazard maps explicitly state their appropriate use and limitations. For example, the geologic hazard and faults maps provided by the City of San Diego [33] explicitly state that “[the] maps do not furnish site specific information and should be used only as a guide when evaluating risk. [The maps] are intended to be an indicator of what to expect at your site and provide general geologic hazard information.” Regardless, information provided by liquefaction hazard maps can still be quite valuable to an engineer performing a site-specific liquefaction hazard evaluation. Because liquefaction hazard maps are typically developed from correlations with surficial geologic units, they can help the engineer to see “the bigger picture” as it relates to the geologic depositional environment of the site, and to understand *why* liquefaction hazard possibly exists. Combining this geologic perspective with site-specific geotechnical data increases the engineer's overall knowledge and understanding of the site, and can help facilitate risk communication to owners, planners, policy-makers, and citizens.

3. Probabilistic analysis methods and reference parameter maps

Site-specific liquefaction triggering and lateral spread hazard assessment using empirical prediction models requires the characterization of seismic loading through the use of the peak ground surface acceleration, a_{max}, earthquake moment magnitude, M, and source-to-site distance, R to represent the design earthquake. The process of selecting these values is relatively straight-forward when analyzing the liquefaction hazard from a single seismic source. However, when analyzing liquefaction hazard from multiple possible seismic sources, the selection of these values becomes more complicated. Seismic hazard in such environments is

commonly characterized with probabilistic seismic hazard analysis (PSHA), which produces a range of possible (M, R) combinations for each return period of a_{max}. Additionally, more recent research [34,35] has demonstrated the importance of considering uncertainty from the local site response in the PSHA when developing the seismic hazard curve for a_{max}.

If using probabilistic ground motions to characterize seismic loading, then liquefaction triggering and lateral spread displacement are commonly evaluated at a single return period with one (M, R) combination assigned to the corresponding probabilistic value of a_{max}. However, liquefaction can also be caused by weaker ground motions that occur more frequently and/or by stronger ground motions that occur more rarely than those associated with the design return period. Despite the many possible (M, R, a_{max}) combinations produced by a PSHA, engineers are faced with the challenge of selecting a single combination that accurately and sufficiently represents the seismic loading at the targeted hazard level. Conventional approaches to selecting these values rely upon the deaggregation results from the PSHA for a_{max} at a targeted return period (termed the "pseudo-probabilistic approach" by Rathe and Saygili [6]). Engineers select either the mean or modal values of M and/or R from the deaggregation, often assuming that their computed liquefaction hazards correspond to the same hazard level or return period as a_{max}. However, many researchers have shown that this assumption is incorrect unless there is zero uncertainty in the response parameter, and that the actual hazard level or return period of the response can vary substantially [5–8].

Potential biases introduced into the liquefaction hazard assessment through the improper and/or incomplete characterization of probabilistic seismic loading can be reduced through the more complete consideration of the seismic loading in a probabilistic liquefaction hazard analysis (PLHA) [36]. For example, consider the probabilistic framework introduced by the Pacific Earthquake Engineering Research Center (PEER) to advance performance-based earthquake engineering design [37–39]. Previous researchers have used this probabilistic framework or others that were similar to evaluate liquefaction triggering potential [5,8,10,40–43], post-liquefaction free-field settlement [44,45], seismic slope stability [6,46,47], lateral spread displacement [7,11], and pile foundation response [48–51].

Unfortunately, the completion of a PLHA is relatively complex and requires multiple probabilistic computations, which can significantly increase project costs. As a result, the approach is rarely applied in routine engineering practice today. Researchers have attempted to address this problem by developing or modifying existing specialized computational tools for probabilistic liquefaction triggering and lateral spread assessment. These computational tools include *LS Displacement Tool* [51,52]; *WSliq* [44,53]; *EZ-FRISK* [54]; and *PBLiquefY* [55]. However, the availability of these tools has not been sufficient for many professionals, who routinely need to perform and/or validate their calculations in a rapid and efficient manner. To address this challenge, researchers developed simplified probabilistic procedures for liquefaction triggering [8–10] and lateral spread displacement [11]. Simplified probabilistic procedures for other hazards such as post-liquefaction free-field settlement and seismic slope displacement are currently in development. These procedures were modeled after the approach taken by the U.S. Geological Survey (USGS) for mapping probabilistic ground motions across the United States using a uniform, reference "bedrock" condition [56].

3.1. Liquefaction and lateral spread reference parameter maps

Simplified probabilistic liquefaction triggering and lateral spread procedures require the use of reference parameter maps that provide uniform hazard estimates of liquefaction-related parameters corresponding to a reference soil profile or soil sublayer. Consider the two soil profiles presented in Fig. 1. The soil profile in Fig. 1(a) presents a reference soil sublayer at a depth of 6 m in saturated sand. The soil profile in Fig. 1(b) presents a reference ground slope soil profile [57] with a zone of liquefiable soil that is 3.0 m thick. Using the reference soil layer shown in Fig. 1(a), Ulmer and Franke [10] demonstrated that a probabilistic liquefaction triggering procedure [5,43] could be applied with the Boulanger and Idriss [58] probabilistic liquefaction triggering model across a grid of geographic points to produce and map probabilistic contours of the median magnitude- and stress-corrected cyclic stress ratio for the reference sublayer at a 6-meter depth, $\widehat{CSR}^{ref}$ at the return period or hazard level of interest. Similarly, using the ground slope soil profile shown in Fig. 1(b), Ekstrom and Franke [11] demonstrated that a probabilistic lateral spread displacement procedure [7,59] could be applied with the Youd et al. [57] empirical lateral spread displacement model to produce and map probabilistic contours of the log-transformed median lateral spread displacement corresponding to the reference soil profile, $\log\left(\widehat{D}_H\right)^{ref}$ at the return period or hazard level of interest.

Probabilistic reference parameter maps for $\widehat{CSR}^{ref}$ were termed *liquefaction loading reference parameter maps* by Ulmer and Franke [10], and reference parameter maps for $\log\left(\widehat{D}_H\right)^{ref}$ were termed *lateral spread reference parameter maps* by Ekstrom and Franke [11]. Using liquefaction loading reference parameter maps and lateral spread reference parameter maps, engineers can obtain reference values of $\widehat{CSR}^{ref}$ and $\log\left(\widehat{D}_H\right)^{ref}$ for their sites corresponding to the return period(s) or hazard level(s) of interest. These reference values can subsequently be corrected for site-specific geotechnical and topographical information to calculate site-specific, uniform hazard estimates of liquefaction factor of

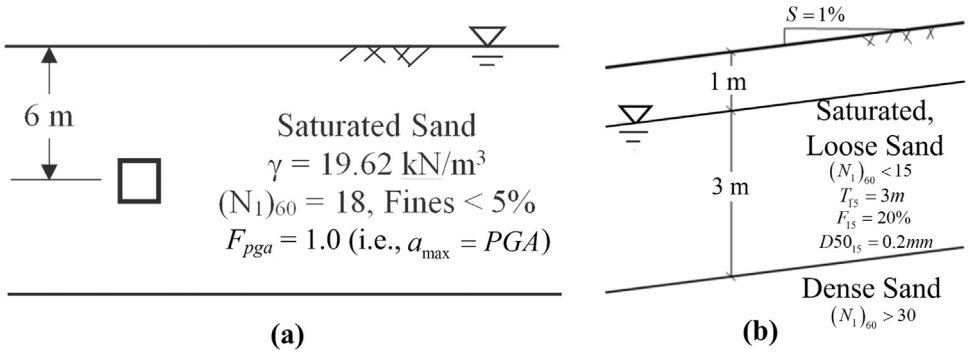

Fig. 1. (a) Liquefaction triggering and (b) lateral spread displacement reference soil profiles used to develop probabilistic reference parameter maps (adapted and modified from Ulmer and Franke [10] and Ekstrom and Franke [11], respectively).

safety, FS_{Liq} with depth and lateral spread displacement at the ground surface, D_H at the return period of interest.

It is important to clarify that the consideration of seismic loading in the development of probabilistic reference parameter maps like those for $\widehat{CSR}^{ref}(\%)$ and $\log\left(\widehat{D}_H\right)^{ref}$ do not rely upon a single scenario earthquake assumption. Every geographic point that is analyzed in the development of a reference parameter map considers a wide range of possible ground motion scenarios across a wide range of hazard levels or return periods. Therefore, ground motions that are both larger than and smaller than those associated with the targeted hazard level are considered, along with their corresponding likelihoods. Such an approach does not incorporate the pseudo-probabilistic assumption by assuming that the hazard level associated with the incorporated ground motion is the same as the resulting computed liquefaction triggering potential and/or lateral spread displacement, but instead computes the return periods associated with liquefaction triggering and/or lateral spread displacement themselves.

4. Clarifying the differences between liquefaction hazard maps and probabilistic reference parameter maps

4.1. Differences in purpose

Traditional liquefaction hazard maps are intended to provide a preliminary indication of potential liquefaction hazards on a regional scale. While these maps are intended to be used as a standalone tool without any geotechnical information regarding the site, the information they provide is too coarse and unreliable to negate the need for a local liquefaction hazard assessment. Probabilistic reference parameter maps are intended to be used for the site-specific assessment of liquefaction triggering and its effects. However, the information provided by probabilistic reference parameter maps is essentially useless without site-specific geotechnical information to accompany it. The reference parameter maps therefore serve as a proxy for the probabilistic seismic loading affecting liquefaction and its effects. Additionally, these maps greatly simplify the process of developing probabilistic liquefaction triggering and lateral spread displacement values by eliminating the need for the engineer to perform numerous iterative probabilistic computations.

4.2. Differences in seismic loading characterization

Traditional liquefaction hazard maps characterize seismic loading with ground motions computed from a deterministic scenario earthquake or from a PSHA at a single hazard level or return period. Maps that incorporate probabilistic ground motions from multiple return periods frequently apply the pseudo-probabilistic assumption. Probabilistic reference parameter maps characterize seismic loading with probabilistic ground motions across all hazard levels or return periods. Reference parameter maps do not apply the pseudo-probabilistic assumption, but are developed through the repeated convolution of the ground motion seismic hazard curves with selected liquefaction fragility relationships to produce reference liquefaction hazard curves at each mapped grid point. Therefore, the reference parameter maps provide a more complete consideration of the probabilistic ground motions affecting liquefaction hazard.

4.3. Differences in hazard level definition

Unless a liquefaction hazard map was developed through the convolution of seismic hazard curves with a series of liquefaction fragility curves, then the hazard level or return period reported on a traditional liquefaction hazard map corresponds to the hazard of the causative ground motion, not necessarily liquefaction itself. The return period or hazard level reported on a probabilistic reference parameter map does not correspond to the causative ground motion, but corresponds to liquefaction itself. When used with site-specific correction factors, a mapped reference parameter value allows characterization of the actual liquefaction or lateral spreading hazard at the targeted return period.

4.4. Differences in vertical variation of liquefaction hazard

Traditional liquefaction hazard maps are two-dimensional representations of a three-dimensional hazard. As such, assumptions must be made regarding the variability of liquefaction with depth to provide a two-dimensional quantification of liquefaction hazard for mapping. Alternatively, a cumulative liquefaction-related damage measure such as LPI can be used to account for the variation of liquefaction with depth. Probabilistic reference parameter maps do not need to account for vertical variations in liquefaction, but they enable engineers to evaluate liquefaction and effects with depth if site-specific geotechnical and topographic information is available.

4.5. The maps are complementary

Traditional liquefaction hazard maps and probabilistic reference parameter maps are two completely different types of maps that serve different purposes. Comparing them is akin to comparing “apples to oranges.” However, like apples and oranges, probabilistic reference parameter maps and traditional liquefaction hazard maps are complementary to one another because each performs a function that the other is unable to perform. Liquefaction hazard maps provide preliminary, regional-scale information to the engineer regarding potential liquefaction hazards before any geotechnical site information is available. This type of information can help the engineer adjust the scope of the site investigation to obtain the necessary information for a thorough site-specific liquefaction assessment [32]. Probabilistic reference parameter maps, when coupled with site-specific geotechnical information, provide localized, hazard-targeted assessment and quantification of liquefaction triggering and/or its effects. If used appropriately, both traditional liquefaction hazard maps and probabilistic reference parameter maps can be used together to help engineers and decision-makers understand and quantify liquefaction hazards at a given site in an objective and a consistent manner.

5. Demonstrative analysis in san diego, california

5.1. Liquefaction hazard map for downtown san diego

To demonstrate how liquefaction hazard maps and probabilistic reference parameter maps can be used together by engineers, an example calculation for a representative site near San Diego Bay, California will be performed. San Diego was selected for this example because of the significant liquefaction triggering potential that exists at locations along San Diego Bay and because of the availability of traditional liquefaction hazard maps, which were developed by the County of San Diego.

The County of San Diego has produced a map of liquefaction hazard for the county as part of the Multi-jurisdictional Hazard Mitigation Plan [60]. A portion of this map focusing on downtown San Diego is presented in Fig. 2. This map was developed using probabilistic peak ground accelerations (2% probability of exceedance in 50 years) from the 2002 USGS update of the National

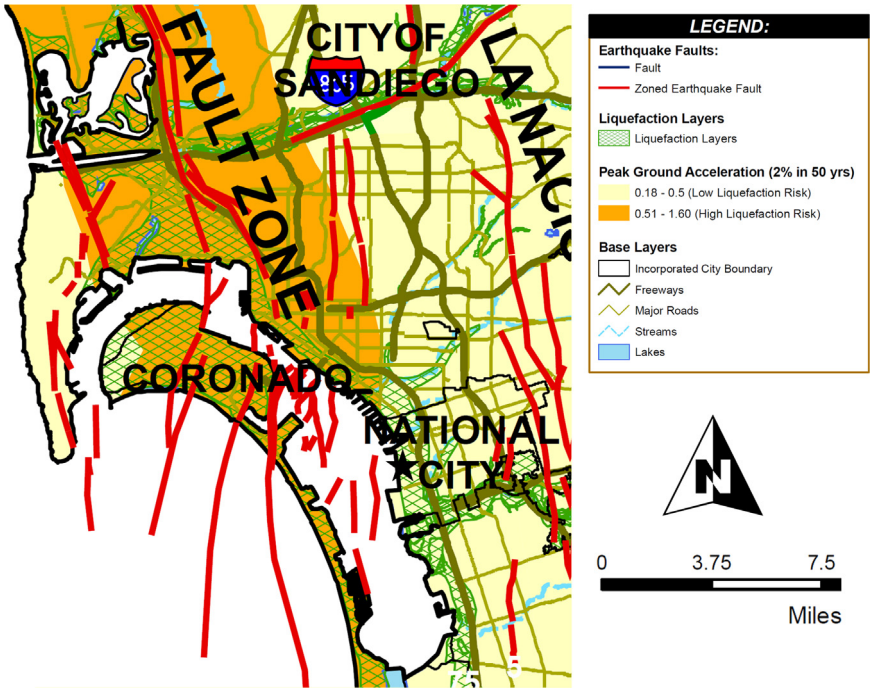

Fig. 2. Liquefaction hazard map of downtown San Diego (adapted from County of San Diego [60]). The star shown on the map represents the location of the representative site.

Seismic Hazard Maps [61], the Scenario Earthquake Shake Map for Rose Canyon fault from the California Integrated Seismic Network (CISN), existing liquefaction areas from local maps, and soil classification from the National Earthquake Hazards Reduction Program (NEHRP). For the purpose of this example, the reader should focus on three particular aspects of the map: (1) the areas where Quaternary alluvial (i.e., susceptible) sediments and a shallow groundwater table are known to exist (labeled as "Liquefaction Layers" in the map legend, and represented by red cross-hatching); (2) the areas where probabilistic ground motions (as computed by Frankel et al. [61]) were mapped between 0.15 g and 0.5 g at a hazard level of 2% probability of exceedance in 50 years (labeled as "Low Liquefaction Risk" in the map legend, and represented by pale yellow coloring on the map); and (3) the areas where probabilistic ground motions were mapped between 0.51 g and 1.60 g at a hazard level of 2% probability of exceedance in 50 years (labeled as "High Liquefaction Risk" in the map legend, and represented by orange coloring on the map.) The descriptors "Low" and "High" associated with liquefaction risk are therefore tied directly to the amplitude of the probabilistic ground motions. Additional features on the map including faults, roads, and streams are described in the map legend, and may be of interest to the reader, but are not necessary for this example problem. Note that the star shown on the map represents the location of the representative site for this example.

5.2. Probabilistic reference parameter maps for downtown san diego

Liquefaction loading parameter maps and lateral spread reference parameter maps corresponding to return periods of 475 and 2475 years were developed for downtown San Diego, California using *PBLiquefY* [55] and *EZ-FRISK* [54] respectively, and are presented in Figs. 3 and 4. USGS probabilistic ground motions developed from the 2008 update of the National Seismic Hazard Maps [56] were used with the full probabilistic procedures [5,7] to create these maps. These maps can be used with site-specific geotechnical information and the site correction factors presented in Appendix A (for liquefaction triggering) and Appendix B (for lateral spread displacement) to develop hazard-targeted (i.e., return periods of 475 and 2475 years) estimates of FS_{Liq} and D_H for any mapped location in downtown San Diego and mapped surrounding areas.

5.3. Representative site and soil profile

Table 1 summarizes a soil profile (to a depth of 17.5 m) and was developed from an actual soil boring performed in the San Diego Bay area. For this example, the soil boring was assumed to be located adjacent to San Diego Bay at a representative site marked by the black star in Fig. 2 through 4. The soil profile generally consists of 1.5 m of unsaturated hydraulic fill, underlain by 10 m of saturated, medium-dense to very dense silty sand (i.e., $(N_1)_{60}$ = 10 – 50+ blows/0.3 m). Depth to groundwater is 1.5 m. An average shear wave velocity of 273 m/s was measured in the upper 30 m at the site, corresponding to an IBC Site Class D [62]. Probabilistic mean peak ground acceleration estimates of 0.179 g and 0.427 g were obtained from the 2008 USGS interactive deaggregation (http://geohazards.usgs.gov/deaggint/2008/, $V_{s,30}$ = 760 m/sec), corresponding to ground motion return periods of 475 and 2,475 years, respectively. Using Table 1613.3.3(1) from the IBC [62], F_{pga} values of 1.442 and 1.073 were interpolated for the ground motion return periods of 475 and 2,475 years, respectively, for a Site Class D. The deaggregation results produce mean moment magnitudes of 6.61 and 6.76 corresponding to return periods of 475 and 2,475 years, respectively. Evaluation of Table 1 suggests that T_{15}^{site} = 3.0 meters (from the poorly-graded sand with silt at depths between 4.5 and 7.5 m, shaded in gray), F_{15}^{site} = 7%, and $D50_{15}^{site}$ = 0.5 mm (assumed for the example). A free-face site geometry with W^{site} = 10% will be assumed for the example.

5.4. Map-based analysis and results

Evaluation of the liquefaction hazard map in Fig. 2 [60] shows that the representative site is located in an area with potential liquefiable layers, denoted by the red cross-hatching on the map.

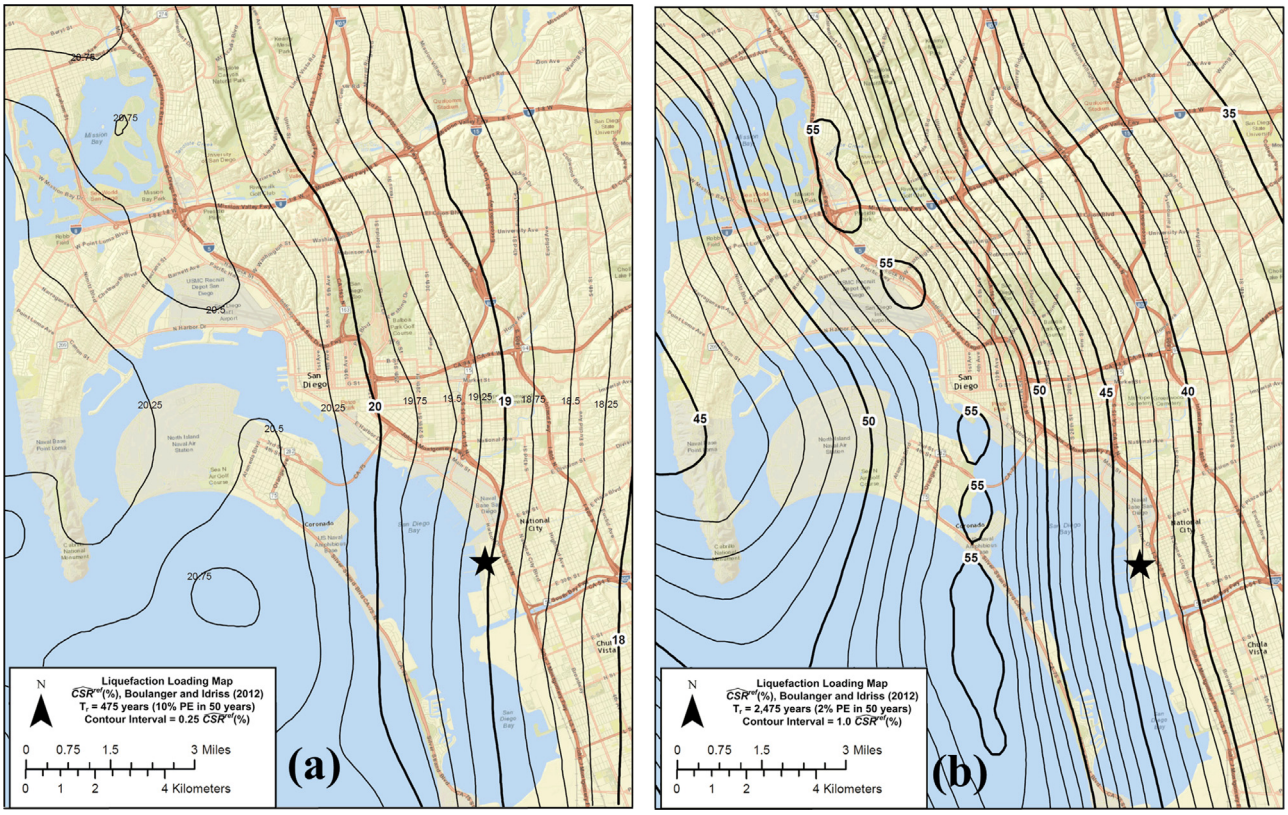

Fig. 3. Probabilistic liquefaction loading reference parameter maps showing $\widehat{CSR}^{ref}(\%)$ for San Diego, California at return periods of (a) 475 years and (b) 2475 years. For use with the Boulanger and Idriss [58] liquefaction triggering model with Idriss and Boulanger (2008, 2010) magnitude scaling factor. The star shown on the maps represents the location of the representative example site near San Diego Bay.

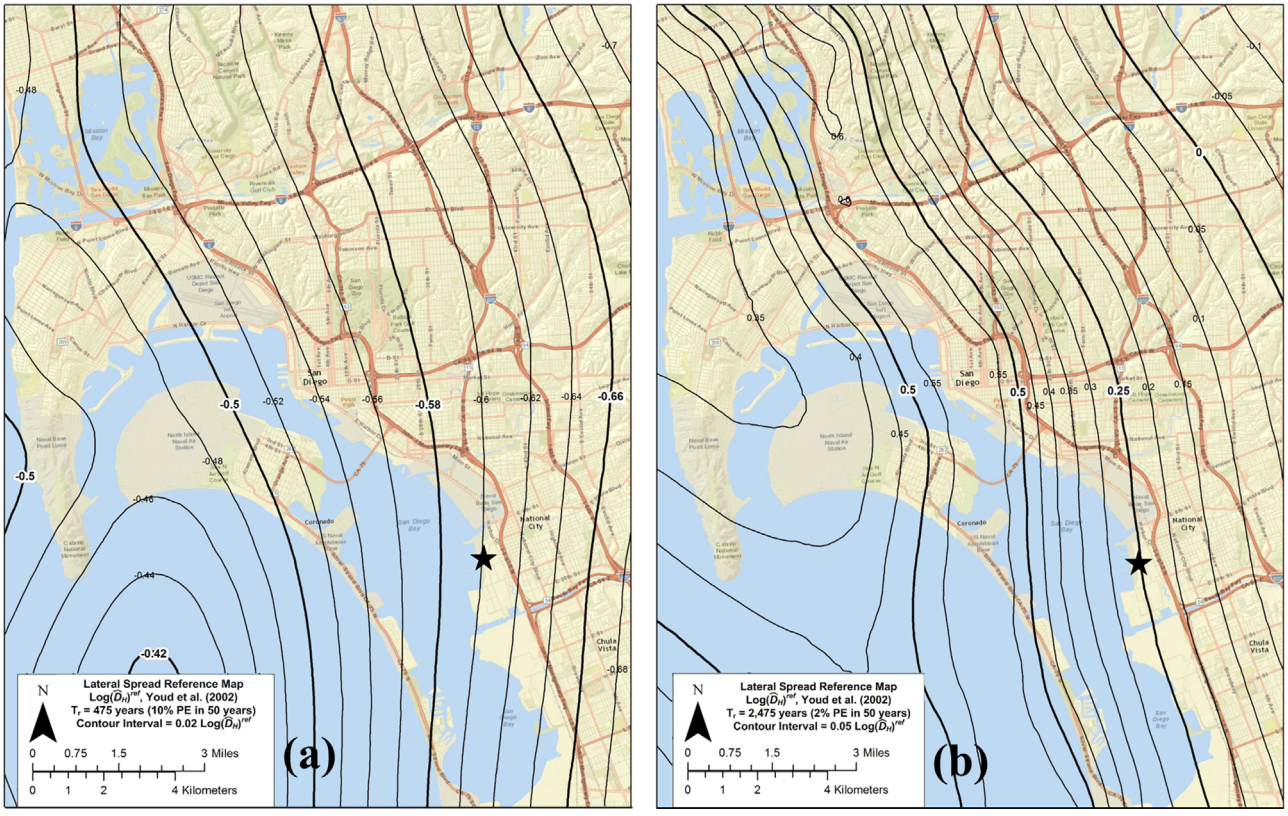

Fig. 4. Probabilistic lateral spread displacement reference parameter maps showing $\log\left(\widehat{D}_H\right)^{ref}$ for San Diego, California at return periods of (a) 475 years and (b) 2475 years. For use with the Youd et al. [57] lateral spreading model. The star shown on the maps represents the location of the representative example site near San Diego Bay.

Table 1
Soil profile for the representative San Diego Bay site.

Depth, z (m)	Soil Type	Thickness (m)	$(N_1)_{60}$ (blows/0.3 m)	Fines (%)	Unit Weight (kN/m^3)	$(N_1)_{60,cs}$ [1] (blows/0.3 m)
0.1	Hydraulic Fill	0.5	12	3	18.70	12.0
0.6	Hydraulic Fill	1.0	20	4	18.70	20.0
1.5	Poorly Graded Sand with Silt	0.5	28	11	18.85	33.6
2.1	Poorly Graded Sand with Silt	1.0	35	12	18.85	37.1
3	Silty Sand	1.5	36	15	19.55	39.3
4.6	Poorly Graded Sand with Silt	1.5	13	8	18.85	13.4
6.1	Poorly Graded Sand with Silt	1.5	14	6	18.85	14.0
7.6	Silty Sand	1.5	36	18	19.55	40.1
9.1	Silty Sand	1.5	43	20	19.55	47.5
10.7	Silty Sand	1.5	50+	17	19.55	54+
12.2	Silty Sand	1.5	50+	23	19.55	55+
13.7	Silty Sand	1.5	50+	24	19.55	55+
15.2	Silty Sand	1.5	50+	22	19.55	55+

Computed using Idriss and Boulanger [20,21]

However, according to the hazard map, the site is located in an area denoted as "Low Liquefaction Risk" due to probabilistic peak ground accelerations (2% probability of exceedance in 50 years) less than 0.5 g. Nevertheless, because the site-specific geotechnical data (i.e., Table 1) suggests that the site may have soil layers that are susceptible to liquefaction, a site-specific liquefaction triggering and lateral spread displacement assessment will be performed.

According to the liquefaction loading parameter maps presented in Fig. 3, the representative site is mapped with probabilistic $\widehat{CSR}^{ref}(\%)$ values of 19.1% and 43.2% at return periods of 475 years and 2475 years, respectively. Table 2 demonstrates how these reference values are used with the correction equations summarized in Appendix A to compute probabilistic estimates of FS_{Liq} with depth. Numbers inside the parentheses correspond to the return period of 2475 years. Note that $\Delta CSR_{MSF} = 0$ because the liquefaction loading parameter maps were developed with the Idriss and Boulanger [20,21] version of the *MSF*. Based on the simplified probabilistic assessment, the FS_L for the poorly-graded sand with silt at depths of 4.5–7.5 m (highlighted in gray) is predicted, on average, to drop below 0.75 every 475 years, and to drop below 0.44 every 2475 years. For additional insight and for the benefit of the reader, the return period of liquefaction (years) for each soil layer was computed with the Kramer and Mayfield [5] procedure (using the Boulanger and Idriss [58] probabilistic liquefaction triggering model for consistency with the simplified probabilistic results), and is shown in Table 2. The return period of liquefaction is defined as the average computed recurrence interval of liquefaction triggering for that soil layer. The return period of liquefaction for the soil layers at depths between 4.5 and 7.5 m ranged between 232 years and 284 years. These return periods are less than the return periods of 475 years and 2475 years that were targeted in the engineering analysis, suggesting that the potential for liquefaction triggering is unacceptably high at this representative site. The reader should also note how these liquefaction return periods differ substantially from the return periods of the input ground motions (i.e., 475 and 2475 years).

Using the lateral spread displacement reference parameter maps presented in Fig. 4, $\log\left(\widehat{D}_H\right)^{ref}$ values of −0.602 and 0.260 are obtained for the representative site, corresponding to return periods of 475 and 2475 years, respectively. The representative site is a free-face geometry case with $W_{15}^{site} = 10\%$ assumed for the example. Using the values of $T_{15}^{site} = 3.0$ meters, $F_{15}^{site} = 7\%$, and $D50_{15}^{site} = 0.5$ mm (assumed), the correction equation presented in Appendix B is used to compute the displacement correction factor $\Delta D_H = 0.075$. With this factor, the site-specific probabilistic estimates of median lateral spread displacement are computed as 0.30 m and 2.16 m for the return periods of 475 and 2475 years, respectively. These values imply that at least 0.30 m of displacement will occur at the representative site every 475 years on average, and at least 2.16 m of displacement every 2475 years on average.

6. Conclusions and limitations

This paper clarified the differences between traditional liquefaction hazard maps and probabilistic reference parameter maps, which are used in simplified probabilistic liquefaction hazard assessments. Traditional liquefaction hazard maps are intended to convey stand-alone information regarding regional liquefaction hazard, and are generally

Table 2
Probabilistic liquefaction triggering results for the representative San Diego Bay site at the return periods of 475 and 2475 years.

Depth, z (m)	USCS	$(N_1)_{60,cs}$ (blows/0.3 m)	ΔCSR_σ (Eqn A2)	$\Delta CSR_{F_{pga}}$ (Eqn A3) 475 (2475)	ΔCSR_{r_d} (Eqn A4) 475 (2475)	ΔCSR_{K_σ} (Eqn A5)	$\widehat{CSR}$ (Eqn A1) 475 (2475)	$\widehat{CRR}$[a]	FS_{Liq} (Eqn A7) 475 (2475)	Return Period of Liquefaction[b] (years)
1.5	SP-SM	33.6	−0.693	0.37 (0.07)	0.08 (0.07)	−0.206	0.121 (0.203)	> 0.6	> 2 (> 2)	> 10,000
2.1	SP-SM	37.1	−0.532	0.37 (0.07)	0.07 (0.06)	−0.219	0.139 (0.233)	> 0.6	> 2 (> 2)	> 10,000
3	SM	39.3	−0.399	0.37 (0.07)	0.05 (0.05)	−0.164	0.166 (0.278)	> 0.6	> 2 (> 2)	> 10,000
4.6	SP-SM	13.4	−0.262	0.37 (0.07)	0.03 (0.03)	0.006	0.219 (0.368)	0.163	0.75 (0.44)	284
6.1	SP-SM	14.0	−0.196	0.37 (0.07)	0.00 (0.00)	0.026	0.232 (0.390)	0.168	0.73 (0.43)	232
7.6	SM	40.1	−0.174	0.37 (0.07)	−0.03 (−0.03)	0.023	0.229 (0.386)	> 0.6	> 2 (> 2)	> 10,000
9.1	SM	47.5	−0.147	0.37 (0.07)	−0.07 (−0.07)	0.068	0.238 (0.402)	> 0.6	> 2 (> 2)	> 10,000
10.7	SM	54	−0.125	0.37 (0.07)	−0.11 (−0.10)	0.112	0.244 (0.413)	> 0.6	> 2 (> 2)	> 10,000
12.2	SM	54	−0.110	0.37 (0.07)	−0.15 (−0.14)	0.149	0.247 (0.420)	> 0.6	> 2 (> 2)	> 10,000
13.7	SM	54	−0.098	0.37 (0.07)	−0.19 (−0.18)	0.184	0.249 (0.423)	> 0.6	> 2 (> 2)	> 10,000
15.2	SM	54	−0.089	0.37 (0.07)	−0.23 (−0.22)	0.216	0.249 (0.425)	> 0.6	> 2 (> 2)	> 10,000

[a] Computed with Boulanger and Idriss [58], P_L=50%
[b] Computed with Kramer and Mayfield [5] procedure using the Boulanger and Idriss [58] model.

developed using mapped surface geology. These maps are not intended to be used in site-specific liquefaction hazard assessment, but as a preliminary screening and zoning resource for engineers and decision-makers. Conversely, probabilistic reference parameter maps provide values of a reference liquefaction hazard or loading parameter that corresponds to a specific reference soil profile, and are intended to be used with site-specific geotechnical and topographical information to develop probabilistic liquefaction hazard estimates at specific return periods. These reference parameter maps are not intended to convey stand-alone information regarding the site. Traditional liquefaction hazard maps and probabilistic reference parameter maps therefore perform very different, but complementary functions.

To demonstrate how traditional liquefaction hazard maps can be used in conjunction with probabilistic reference parameter maps, a liquefaction triggering and lateral spread displacement assessment is performed for a representative site near San Diego Bay, California. Liquefaction loading reference parameter maps and lateral spread displacement reference parameter maps for San Diego are developed at return periods of 475 years (i.e., 10% probability of exceedance in 50 years) and 2475 years (i.e., 2% probability of exceedance in 50 years). Correction equations necessary to use the reference parameter maps for the assessment of liquefaction triggering and lateral spread displacement are summarized in the appendix. In the example, the liquefaction hazard map suggests that the site might have liquefiable layers, but possibly low levels of ground motions to induce liquefaction triggering. The subsequent simplified probabilistic liquefaction triggering analysis shows that liquefaction would likely trigger in a soil layers located between 4.5 and 7.5 m below the ground surface at both the return periods of 475 and 2475 years. A simplified probabilistic lateral spread displacement assessment suggests displacements of 0.3 m and 2.16 m for the return periods of 475 and 2475 years, respectively.

As noted by Mayfield et al. [8] and Franke et al. [9], the intent of a simplified probabilistic procedure is to make possible for practicing engineers the realization of a PLHA on routine projects without the need of lengthy probabilistic calculations. However, probabilistic procedures, like all others, require thorough characterization and careful interpretation of subsurface conditions for proper evaluation of liquefaction hazards. A sophisticated probabilistic analysis does not compensate for inadequate geotechnical data or inaccurate subsurface interpretations.

Acknowledgments

The authors would like to thank Professors Steven L. Kramer (University of Washington), T. Leslie Youd (Brigham Young University, Emeritus), and Daniel T. Gillins (Oregon State University) for their preliminary reviews of this paper. Their comments and suggestions were both insightful and helpful. Funding for this study was provided in part by a Federal Highway Administration Transportation Pooled Fund Study (Award No. TPF-5(296), with participation for Utah, Alaska, Connecticut, Idaho, Montana, South Carolina, and Oregon state departments of transportation) and a grant from the U.S. Geological Survey External Research Program (Award No. G14AP00031). We gratefully acknowledge this support. However, the conclusions and opinions expressed in this paper do not necessarily reflect those of our sponsors.

Appendix A. Site-specific correction equations for liquefaction triggering

To compute uniform-hazard estimates of the median magnitude- and stress-corrected cyclic stress ratio, $\widehat{CSR}_{M=7.5,\sigma_v'}=1atm$ mapped reference values of $\widehat{CSR}^{ref}$ must be corrected for local soil conditions. For convenience in interpolation, liquefaction loading maps typically plot $\widehat{CSR}^{ref}$ as a percent (i.e., $\widehat{CSR}^{ref}(\%)$). According to the Ulmer and Franke [10], simplified probabilistic procedure that incorporates the Boulanger and Idriss (2012) probabilistic liquefaction triggering model, $\widehat{CSR}_{M=7.5,\sigma_v'}=1atm$ for a given soil layer i can be computed as:

$$\left(\widehat{CSR}_{M7.5,\sigma_v'=1atm}\right)_i=\widehat{CSR}_i = \exp\left[\begin{array}{l}\ln\left(\dfrac{\widehat{CSR}^{ref}(\%)}{100}\right)+(\Delta CSR_{\sigma})_i+\left(\Delta CSR_{F_{pga}}\right)_i+\left(\Delta CSR_{r_d}\right)_i\\ +(\Delta CSR_{MSF})_i+\left(\Delta CSR_{K_\sigma}\right)_i\end{array}\right] \quad (A.1)$$

where $(\Delta CSR_{\sigma})_i$, $(\Delta CSR_{F_{pga}})_i$, $(\Delta CSR_{r_d})_i$, $(\Delta CSR_{MSF})_i$, and $(\Delta CSR_{K_\sigma})_i$ are site-specific correction factors for soil stress, stress reduction, magnitude scaling factor, and overburden pressure, respectively, for soil layer i. If a liquefaction loading map was developed using the reference soil sublayer shown in Fig. 1(a), then these correction factors are given as:

$$(\Delta CSR_{\sigma})_i=\ln\left[\frac{(\sigma_v/\sigma_v')_i}{(\sigma_v/\sigma_v')^{ref}}\right]=\ln\left[\frac{(\sigma_v/\sigma_v')_i}{2}\right] \quad (A.2)$$

$$\left(\Delta CSR_{F_{pga}}\right)_i=\ln\left(\frac{F_{pga}\cdot PGA_{rock}}{F_{pga}^{ref}\cdot PGA_{rock}}\right)=\ln\left(\frac{F_{pga}}{1}\right)=\ln\left(F_{pga}\right) \quad (A.3)$$

$$\left(\Delta CSR_{r_d}\right)_i=\ln\left(\frac{r_{d,i}}{r_d^{ref}}\right)=\left(-0.6712-1.126\sin\left(\frac{z}{11.73}+5.133\right)\right) +\overline{M}\left(0.0675+0.118\sin\left(\frac{z}{11.28}+5.142\right)\right) \quad (A.4)$$

$$\left(\Delta CSR_{K_\sigma}\right)_i=-\ln\left(\frac{K_{\sigma,i}}{K_\sigma^{ref}}\right) -\ln\left(\frac{1-MIN\left\{\dfrac{0.3}{\dfrac{1}{18.9-2.55\sqrt{\left[(N_1)_{60,cs}\right]_i}}}\right\}\cdot\ln\left(\dfrac{(\sigma'_v)_i}{p_a}\right)}{1.067}\right) \quad (A.5)$$

where $(\sigma_v)_i$ is the total stress for soil layer i; $(\sigma_v')_i$ is the effective stress for soil layer i (in the same units as $(\sigma_v)_i$); F_{pga} is the site-specific site amplification factor for the peak ground acceleration (PGA) corresponding to "bedrock" (i.e., $V_{s,30}=760$ m/sec) obtained by seismic code, an empirical relationship (e.g., Stewart et al. [63]), or a site response analysis; z is the soil depth below the ground surface (in meters); $\bar{M}$ is the mean deaggregated moment magnitude of the PGA at the target return period or hazard level; and p_a is atmospheric pressure (in the same units as $(\sigma_v')_i$).

The magnitude scaling correction factor for soil layer i, (ΔCSR_{MSF}) shown in Equation (A.1) depends upon which version of the Boulanger and Idriss magnitude scaling factor the liquefaction loading map was developed with. If the liquefaction loading map and corresponding $\widehat{CSR}^{ref}$ values were developed with the Idriss and Boulanger [20,21] recommended MSF, then the MSF remains constant and is the same for both the reference soil layer and the actual soil layer (i.e., $MSF^{ref}=(MSF^{site})_i$). Therefore, if using the Idriss and Boulanger [20,21] version of the MSF, $(\Delta CSR_{MSF})_i=0$. However, if the liquefaction loading map was developed with the updated MSF presented by Boulanger and Idriss [64], then

$MSF^{ref} \neq (MSA^{site})_i$, and $(\Delta CSR_{MSF})_i$ is calculated as:

$$(\Delta CSR_{MSF})_i = -\ln\left[\frac{MSF_i}{MSF^{ref}}\right] = -\ln\left(\frac{1 + MIN\left\{\left(\frac{(N_1)_{60,cs})_i}{31.5}\right)^2 + 0.09,\ 1.2\right\}\cdot\left(8.64\cdot\exp\left(\frac{-M}{4}\right) - 1.325\right)}{3.603\cdot\exp\left(\frac{-M}{4}\right) + 0.447}\right) \quad (A.6)$$

Once $(\widehat{CSR}_{M=7.5,\sigma'_v=1atm})_i$ is calculated for soil layer i using Equation (A.1), then the site-specific probabilistic FS_{Liq} for soil layer i can be computed with the median (i.e., $P_L = 50\%$) cyclic resistance ratio, $\widehat{CRR}$ [58] as:

$$(FS_{Liq})_i = \frac{\exp\left[\left(\frac{[(N_1)_{60,cs}]_i}{14.1}\right) + \left(\frac{[(N_1)_{60,cs}]_i}{126}\right)^2 - \left(\frac{[(N_1)_{60,cs}]_i}{23.6}\right)^3 + \left(\frac{[(N_1)_{60,cs}]_i}{25.4}\right)^4 - 2.67\right]}{\widehat{CSR}_i} \quad (A.7)$$

It is important to clarify that the simplified probabilistic liquefaction triggering procedure summarized here does not explicitly account for uncertainty in the site amplification, but rather just considers the median estimated site amplification factor as specified by code or as computed with a site-specific site response analysis or empirical model. Neglecting the uncertainty in site amplification can potentially under-predict the actual liquefaction triggering hazard. The reader is referred to Ulmer and Franke [10] for additional discussion on this point and some possible solutions to incorporate site amplification uncertainty into the simplified probabilistic approach.

The simplified probabilistic liquefaction triggering procedure summarized here incorporates in-situ SPT resistance to quantify liquefaction triggering resistance. However, probabilistic liquefaction triggering assessment could be performed using any other in-situ site characterization method (e.g., cone penetration test (CPT) and shear wave velocity testing) for which probabilistic liquefaction triggering models are available. Therefore, similar simplified probabilistic liquefaction triggering procedures could also be developed and validated for these other in-situ site characterization methods through future research.

Appendix B. site-specific correction equations for lateral spreading displacement

To develop site-specific, hazard-targeted estimates of lateral spread displacement, uniform-hazard values of $(\log \widehat{D_H})^{ref}$ from a lateral spread reference parameter map can be corrected for site-specific soil and topographic information [11]. If the lateral spread reference parameter map was developed using the reference ground slope soil profile shown in Fig. 1(b), then the site-specific, uniform-hazard lateral spread displacement, D_H^{site} can be computed as:

$$D_H^{site} = 10^{\left(\left[\log \hat{D}_H\right]^{ref} + \Delta D_H\right)} \quad (B.1)$$

$$\Delta D_H = 9.044 + b_0^{site} + b_4^{site}\log\left(W^{site}\right) + b_5^{site}\log\left(S^{site}\right) + 0.540\log T_{15}^{site} + 3.413\log\left(100 - F_{15}^{site}\right) - 0.795\log\left(D50_{15}^{site} + 0.1\right) \quad (B.2)$$

where b_0^{site}, b_4^{site}, and b_5^{site} represent model coefficients and are presented in Table B.1; W^{site} is the free-face ratio (in percent) and is computed as the ratio of the vertical distance to the horizontal distance from the site to the free-face toe; S^{site} is the ground slope of the site (in percent); T_{15}^{site} is the cumulative thickness of susceptible liquefiable soil with corrected SPT resistance $(N_1)_{60} < 15$ (in meters); F_{15}^{site} is the average fines content (in percent) for the soil layers comprising T_{15}^{site}; and $D50_{15}^{site}$ is the mean grain size diameter (in mm) of the soil layers comprising T_{15}^{site}.

Table B.1
Site-specific model coefficients for computing the adjustment factor, ΔD_H.

Model	b_0^{site}	b_4^{site}	b_5^{site}
Ground-Slope	−16.213	0	0.338
Free Face	−16.713	0.592	0

References

[1] Youd TL, Hoose SN. Liquefaction susceptibility and geologic setting. 6th World Conf Earthq Eng 1977:2189–94.
[2] Youd TL, Perkins DM. Mapping liquefaction-induced ground failure potential. J. Geotechnical Eng, 104. ASCE,; 1978. p. 433–46.
[3] Power MS, Holzer TL. Liquefaction Maps. Techbrief 1. Appl Tech Counc, Redw City, CA 1996:12.
[4] Holzer TL. Theme (paper -) Probabilistic liquefaction hazard mapping. Geotech. Earthquake ENG. Soil Dyn. IV, GSP 181.Reston, VA: ASCE,; 2008.
[5] Kramer SL, Mayfield RT. Return period of soil liquefaction. J Geotech Geoenviron Eng, 133. ASCE,; 2007. p. 802–13.
[6] Rathje EM, Saygili G. Probabilistic seismic hazard analysis for the sliding displacement of slopes: scalar and vector approaches. J Geotech Geoenviron Eng, 134. ASCE,; 2008. p. 804–14.
[7] Franke KW, Kramer SL. A procedure for the empirical evaluation of lateral spread displacement hazard curves. J Geotech Geoenviron Eng, ASCE 2014;140 (1):110–20.
[8] Mayfield RT, Kramer SL, Huang YM. Simplified approximation procedure for probabilistic evaluation of liquefaction potential. J Geotech Geoenviron Eng, ASCE, 136; 2010. p. 140–50.
[9] Franke KW, Mayfield RT, Wright AD. Simplified uniform hazard liquefaction analysis for bridges. Trans Res Rec, TRB 2014;2407:47–55. http://dx.doi.org/10.3141/2407-05.
[10] Ulmer KJ, Franke KW. A modified probabilistic liquefaction triggering procedure using liquefaction loading parameter maps. J Geotech Geoenviron Eng, ASCE 2016;142(3) 10.106/(ASCE)GT.1943–5606.0001421, 04015089.
[11] Ekstrom LT, Franke KW. A simplified procedure for the probabilistic prediction of lateral spread displacements. J Geotech Geoenviron Eng, ASCE, 142; http://dx.doi.org/10.1061/(ASCE)GT.1943–5606.0001440, 04016028.
[12] Kramer SL. Geotechnical Earthquake Engineering.Upper Saddle River, NJ: Prentice-Hall, Inc,; 1996. p. 653.
[13] Anderson LR, Keaton JR, Aubry K, Ellis SJ. Liquefaction Potential Map for Davis County, Utah, U.S. Geological Survey Contract Report 94-2, Golden, CO, 50; 1994. p.
[14] Baise LG, Higgins RB, Brankman CM. Liquefaction hazard mapping–Statistical and spatial characterization of susceptible units. J Geotech Geoenviron Eng, ASCE, 132; 2006. p. 705–15.
[15] Lenz JA, Baise LG. Spatial variability of liquefaction potential in regional mapping using CPT and SPT Data. Soil Dyn Earthquake Eng 2007;27:690–702.
[16] Gillins DT. Mapping the probability and uncertainty of liquefaction-induced ground failure (PhD Dissertation).UT: Univ. of Utah, SALT Lake City,; 2012. p. 177.
[17] Seed HB, Idriss IM. Simplified procedure for evaluating soil liquefaction potential. J Soil Mech Found Div., ASCE, 97; 1971. p. 1249–73.
[18] Youd TL, et al. Liquefaction resistance of soils: Summary report from the 1996 NCEER and 1998 NCEER/NSF workshops on evaluation of liquefaction resistance of soils. J Geotech Geoenviron Eng, ASCE, 127; 2001. p. 817–33.
[19] Cetin KO, Seed RB, Der Kiureghian A, Tokimatsu K, Harder Jr. LF, Kayen RE, Moss RES. SPT-based probabilistic and deterministic assessment of seismic soil liquefaction potential. J Geotech Geoenviron Eng, ASCE 2004;130(12):1314–40.
[20] Idriss IM, Boulanger RW. Soil liquefaction during earthquakes. Monograph MNO-12 Oakland: Earthquake Engineering Research Institute,; 2008 CA 261 pp.
[21] Idriss IM, Boulanger RW. SPT-based liquefaction triggering procedures. Rep. UCD/CGM-10/02.Davis, CA: Dept. of Civil and Environmental Engineering, Univ. of California–Davis,; 2010.
[22] Iwasaki T, Tokida K, Tatsuoka F, Watanabe S, Yasuda S, Sato H. Microzonation

for soil liquefaction potential using simplified methods. 3rd International Earthquake Microzonation Conf., 1982, 1319–1330.
[23] Luna R, Frost DJ. Spatial liquefaction analysis system. J Computing in Civil Eng, 12. ASCE,; 1998. p. 48–56.
[24] Holzer TL, Bennett MJ, Noce TE, Padovani AC, Tinsley III JC. Liquefaction hazard mapping with LPI in the greater Oakland, California, area. Earthq Spectra 2006;22(3):693–708.
[25] Cramer CH, Rix GJ, Tucker K. Probabilistic liquefaction hazard maps for Memphis, Tennessee. Seism Res Lett, SSA 2008;79(3):416–23.
[26] Lee D-H, Ku C-S, Yuan H. A study of the liquefaction risk potential at Yuanlin, Taiwan. Engr. Geology, Elsevier, 71; 2003. p. 97–117.
[27] Sonmez H, Gokceoglu C. A liquefaction severity index suggested for engineering practice. Env Geol 2005;48(1):81–91.
[28] Olsen MJ, Bartlett SF, Solomon BJ. Lateral spread hazard mapping of the Northern Salt Lake Valley, Utah, for a M7.0 scenario earthquake. Earthq Spectra 2007;23(1):95–113.
[29] Youd TL, Perkins DM. Mapping of liquefaction severity index. J Geotechnical Eng ASCE, 113; 1987. p. 1374–92.
[30] Mabey MA, Madin IP, Youd TL, Jones CF. Earthquake hazards of the Portland quadrangle, Multnomah and Washington Counties, Oregon, and Clark County, Washington. Geological Map Series GMS-79.Portland, OR: Oregon Dept. Geology and Mineral Industries,; 1993.
[31] Jaimes MA, Nino M, Reinoso E. Regional map of earthquake-induced liquefaction hazard using the lateral spreading displacement index DLL. Nat. Hazards, Springer. http://dx.doi.org/10.1007/s1069-015-1666-1.
[32] Southern California Earthquake Center (SCEC), 1999. Recommended Procedures for Implementation of DMG Special Publication 117, Guidelines for Analyzing and Mitigating Liquefaction Hazards in California. University of Southern California, Los Angeles, CA.
[33] City of San Diego, 2008. The San Diego Seismic Safety Study, ⟨http://www.sandiego.gov/development-services/industry/hazards/index.shtml⟩.
[34] Bazzurro P, Cornell CA. Ground motion amplification in nonlinear soil sites with uncertain properties. Bull Seismol Soc Am, SSA 2004;94(6):2090–109.
[35] Stewart JP, Afshari K, Hashash YMA. Guidelines for performing hazard-consistent one-dimensional ground response analysis for ground motion prediction. PEER Report 2014/16.Berkeley, CA: Pacific Earthquake Engineering Research Center,; 2014. p. 117.
[36] Franke KW, Lingwall BN, Youd TL. The sensitivity of empirical liquefaction assessment to seismic loading in areas of low seismicity and its implications for sustainability. Geo-Congress 2014, Geo-Characterization and Modeling for Sustainability, GSP 234, ASCE, 2014 1284–1293.
[37] Cornell CA, Krawinkler H. Progress and challenges in seismic performance assessment. (PEER News). Pacific Earthquake Engineering Research Center,; 2000. p. 1–3.
[38] Krawinkler H. A general approach to seismic performance assessment. Int. Conf. on Advances in New Challenges in Earthquake Engineering Research, ICANCEER, Hong Kong, China. 2002.
[39] Deierlein GG, Krawinkler H, Cornell CA. A framework for probabilistic earthquake engineering. 2003 Pacific Conference on Earthquake Engineering, Wellington, New Zealand. 2003.
[40] Marrone J, Ostadan F, Youngs R, Itemizer J. Probabilistic liquefaction hazard evaluation: Method and application. 17th Int. Conf. Struct. Mech. in Reactor Tech. (Smart 17), Prague, Czech Republic, Paper No. M02-1. 2003.
[41] Juang CH, Li DK, Fang SY, Liu Z, Khor EH. Simplified procedure for developing joint distribution of a_{max} and M_w for probabilistic liquefaction hazard analysis. J. Geotech. Geoenviron. Eng, ASCE, 134; 2008. p. 1050–8.
[42] Baker JW, Faber M. Liquefaction risk assessment using geostatistics to account for soil spatial variability. J. Geotech. Geoenviron. Eng, ASCE, 134; 2008. p. 14–23.
[43] Franke KW, Wright AD, Ekstrom LT. Comparative study between two probabilistic liquefaction triggering models for the standard penetration test. J. Geotech. Geoenviron. Eng, ASCE, 140; 2014. p. 04014010.
[44] Huang Y-M. Probabilistic design and Evaluation for liquefaction-related seismic hazards (PhD Dissertation). Seattle, WA.: Univ. of Washington,; 2008. p. 376.
[45] Kramer SL, Huang YM, Greenfield MW. Probabilistic assessment of Liquefaction Hazards. Geotechnics for Catastrophic Flooding Events. ISBN 978-1-138-02709-1. In: Iai, editor. London: Taylor and Francis Group; 2014. p. 17–26.
[46] Travasarou T, Bray JD, Kiureghian A Der, 2004. A probabilistic methodology for assessing seismic slope displacements. 13th World Conf. on Earthquake Eng., IAEE, Paper No. 2326, Tokyo, Japan.
[47] Rathje EM, Saygili G. Estimating fully probabilistic seismic sliding displacements of slopes from a pseudoprobabilistic approach. J. Geotech. Geoenviron. Eng, ASCE, 137; 2011. p. 208–17.
[48] Ledezma C, Bray JD. Probabilistic probabilistic procedure to evaluate pile foundations at sites with liquefaction-induced lateral displacement. J. Geotech. Geoenviron. Eng, ASCE, 136; 2010. p. 464–76.
[49] Brandenberg SJ, Kashighandi P, Zhang J, Huo Y, Zhao M. Fragility functions for bridges in liquefaction-induced lateral spreads. Earthq Spectra 2011;27(3):683–717.
[50] Bradley BA, Cubrinovski M, Haskell JJM, 2011. Probabilistic pseudo-static analysis of pile foundations in liquefiable soils. Soil Dynamics and Earthquake Eng., Elsevier, 31, 1414-1425.
[51] Franke KW. A probabilistic model for the computation of kinematic pile response due to lateral spread and its application on select bridges damaged during the M7.6 earthquake in the Limon Province, Costa Rica (PhD Dissertation). Provo, UT: Brigham Young University,; 2011. p. 437.
[52] Franke KW. Development of a probabilistic model for prediction of lateral spreading displacements (M.S. Thesis). Seattle, WA: Univ. of Washington,; 2005. p. 294.
[53] Kramer SL. Evaluation of liquefaction hazards in Washington State. Report WA-RD 668.1. Washington State Dept. of Transportation,; 2008. p. 152.
[54] EZ-FRISK 7.60 [Computer Software]. Boulder, CO, Risk Engineering.
[55] Franke KW, Wright AD, Hatch CK, 2014. PBLiquefY: A new analysis tool for the probabilistic evaluation of liquefaction triggering. 10th Nat. Conf. Earthquake Eng., Paper No. 87, EERI, Oakland, CA.
[56] Petersen MD, Frankel AD, Harmsen SC, Mueller SC, Haller KM, Wheeler RL, et al., 2008. Documentation for the 2008 Update of the United States National Seismic Hazard Maps. USGS Open-File Report 2008–1128. 128 pp.
[57] Youd TL, Hansen CM, Bartlett SF. Revised multilinear regression equations for prediction of lateral spread displacement. J. Geotech. Geoenviron. Eng, ASCE, 128; 2002. p. 1007–17.
[58] Boulanger RW, Idriss IM. Probabilistic standard penetration test-based liquefaction-triggering procedure. J Geotech Geoenviron Eng, ASCE 2012:1185–95. http://dx.doi.org/10.1061/(ASCE)GT.1943–5606.0000700.
[59] Kramer SL, Franke KW, Huang Y-M, Baska D, 2007. Probabilistic evaluation of lateral spreading displacement. 4th International Conf. Earthquake Geotech. Eng., (Paper No). 1208, (Thessaloniki, Greece).
[60] County of San Diego, 2007. Draft – Liquefaction County of San Diego Hazard Mitigation Planning, ⟨http://www.sandiegocounty.gov/oes/docs/DRAFT_COSD_Liquefaction1.pdf⟩.
[61] Frankel AD, Petersen MD, Mueller CS, Haller KM, Wheeler RL, Leyendecker EV, Wesson RL, Harmsen SC, Cramer CH, Perkins DM. KS Rukstales, 2002. Documentation for the 2002 Update of the National Seismic Hazard Maps, USGS Open File Report 02-420, (Denver, CO).
[62] International Building Code, 2014. International Building Code ISBN: 978-1-60983-468-5. IL: International Code Council, Inc., Country Club Hills,; 2015.
[63] Stewart JP, Liu AH, Choi Y. Amplification factors for spectral acceleration in tectonically active regions. Bull Seismol Soc Am 2003;93(7):332–52.
[64] Boulanger RW, Idriss IM. CPT and SPT based liquefaction triggering procedures. Rep. UCD/CGM-14/01.Davis, CA: Dept. of Civil and Environmental Engineering, Univ. of California–Davis,; 2014.